PHYSICAL REVIEW A VOLUME 24, NUMBER 3 SEPTEMBER 1981

Prompt and time-delayed electron decay-in-flight spectra of gas-excited carbon ions

D. Schneider and R. Bruch*
Hahn-Meitner-Institut für Kernforschung Berlin GmbH, Bereich Kern- und Strahlenphysik, D-1000 Berlin 39, West Germany

W. Butscher and W. H. E. Schwarz
Theoretische Chemie, Universität Siegen, D-5900 Siegen, West Germany

(Received 24 September 1980)

Auger-electron emission from 400-keV carbon ions excited in single gas collisions with CH_4, Ne, and Ar has been investigated. Prompt and time-delayed projectile electron-emission spectra have been measured, and spectroscopic assignments are given. Absolute inner-shell vacancy-production cross sections and relative line intensities deduced from the prompt and time-delayed spectra for excited carbon ions have been compared as a function of exciter gases. An enhanced probability for electron excitation into high-spin states in carbon is found. Especially for the collision system $C^+ \rightarrow Ne$, a striking population of the $1s2s2p\ ^4P^o$ quartet state relative to the berylliumlike quintet and boronlike sextet states is observed. It is assumed that this is accounted for by cascade-feeding mechanisms. In particular, cascades from Rydberg levels feeding the C IV $1s2s2p\ ^4P^o$, C III $1s2s2p^2\ ^5P$, and C II $1s2s2p^3\ ^6S^o$ high-spin states are discussed. Finally, wavelengths associated with electric dipole ($E1$) transitions among quintet terms in C III and sextet terms in C II are predicted using *ab initio* methods.

I. INTRODUCTION

Little is known experimentally and theoretically about cascade-induced repopulation of multiply excited states with high orbital, spin, and angular-momentum quantum numbers. Such states are often created with surprisingly large cross sections by the beam-foil or beam-gas interaction.[1-6] Recent progress in beam-foil[7] and beam-gas[8-10] electron spectroscopy offers the possibility to study excitation and deexcitation mechanisms for highly excited ionic projectile states via the Auger decay.[11] This time-of-flight technique allows one to analyze the decay of long-lived metastable autoionizing states which are frequently populated by a sequence of cascades that incorporates optical and Auger transitions.

We report here on electron emission spectra[12] from highly ionized carbon projectile ions using various gas targets (CH_4, Ne, and Ar) and a fixed impact energy. The variation of exciter games gives different probabilities for electron excitation into high-lying orbitals and this in turn has a different influence on "cascade-feeding" mechanisms. Such mechanisms have previously been suggested to account for an overpopulation of $1s2s^2$ and $1s2s2p$ configurations relative to $1s2p^2$ initial configurations in highly ionized neon.[13] The influence of cascade-feeding processes for a repopulation of highly excited states in highly stripped recoil ions via selective electron-capture processes has been pointed out only recently.[14]

In Sec. II, the experimental setup is described. To assign the observed structures, excitation energies for a series of core-excited states have been calculated using the generalized-Brillouin-theorem–multiconfiguration method (GBTMC) of Schwarz and Chang (see Sec. III). The spectroscopic assignment is given in Sec. IV. In Sec. V total and relative K-shell excitation cross sections are discussed and possible types of cascade-feeding mechanisms are suggested. Finally, in Sec. VI we present for the first time Grotrian diagrams for C III quintet and C II sextet states.

II. EXPERIMENTAL

In this work high-resolution electron decay-in-flight spectra of highly ionized carbon ions produced by 400-keV-C^+ ion beams excited in CH_4, Ne, and Ar gas targets were studied. Prompt as well as time-delayed electron emission spectra have been measured using the technique of Auger-electron spectroscopy in a crossed-beam apparatus as described previously in more detail.[15] In order to obtain time-delayed spectra, the jet for the injection of the target gas was moved upstream. With a jet and a turbomolecular pump with a pumping speed of about 200 l/s underneath the jet, a fairly narrow scattering region of about 3 mm thickness and 5×10^{-3}-Torr density was maintained. For carbon no appreciable fractions of neutral berylliumlike and lithiumlike ionic states are present in the incoming beam of C^+. We further note that core-excited metastable states are very unlikely to be created in the ion source. It should, however, be pointed out that escape of target gas in the beam direction may lead to a small residual pressure close to the viewing region of the electron spectrometer. On the other hand, our data confirm that contaminations from prompt transitions in the time-delayed

spectra are negligible. Similarly, the fraction of states due to multiple collisions is expected to be small.

The flight path for a time delay of 12 ns is about 3 cm at 400 keV. The pressure in the collision region was low enough to ensure single-collision conditions. Electrons ejected from the gas-excited carbon beam were analyzed by a parallel-plate electrostatic spectrometer. The basic resolution was 2.6% full width at half maximum (FWHM). For spectroscopic studies this resolution could be improved by deceleration of the incident electrons as described previously.[16] Small observation angles with respect to the ion-beam axis were chosen to reduce kinematic broadening effects.[9,15,17] Representative spectra are displayed in Fig. 1. For each gas target a prompt spectrum is compared to a delayed spectrum taken at a laboratory-emission angle Θ_L of 18° and a time delay of about 12 ns. The spectra are plotted in the ionic rest frames.

III. THEORETICAL

In order to interpret our data, excitation and auger-transition energies associated with highly excited carbon ions have been determined theoretically. Thus energies of a series of core-excited states have been calculated by GBTMC techniques as described in Ref. 10 (see also Refs. 7, 18, and 19). A ($15s9p4d$, $11s7p4d$) contracted Gaussian-lobe basis set with orbital exponents down to 0.01 was used. Internal and semi-internal correlations were explicitly taken into account in the

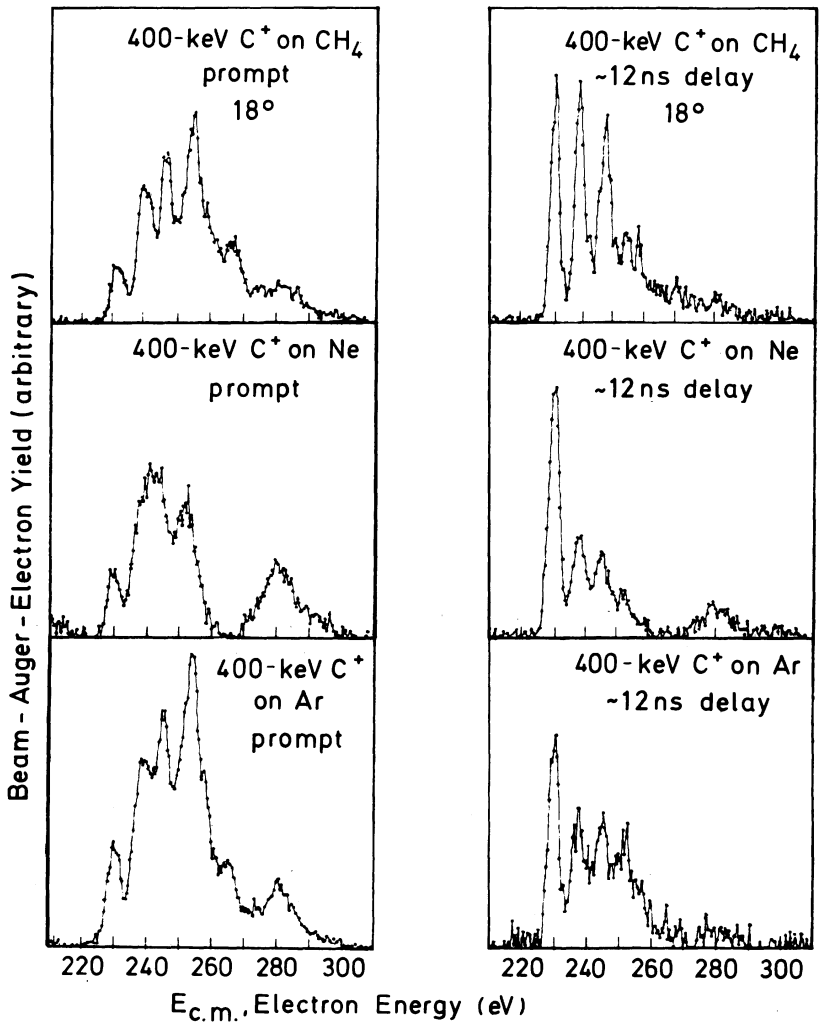

FIG. 1. Prompt and time-delayed electron decay in flight spectra from 400-keV carbon projectile ions highly excited in different gas targets.

TABLE I. Calculated energy values of some prominent high-spin states in carbon (energies are given in eV). Relativistic corrections are not included.

Initial charge state	Main configuration	Term	Energy[a] (eV)	Other authors
C	$1s2s2p^3 3s$	$^7S^o$	736.2	
C^+	$1s2s2p^3$	$^6S^o$	732.22	731.08 (Ref. 23)
C^+	$1s2s2p^2 3s$	^6P	711.86	
C^+	$1s2s2p^2 3p$	$^6S^o$	709.2	
		$^6P^o$	709.7	
		$^6D^o$	709.9	
C^+	$1s2s2p^2 3d$	^6P	707.3	
		^6D	707.2	
		^6F	707.4	
	$1s2p^3 3p$	^6P	697.65	
C^{2+}	$1s2s2p^2$	^5P	701.06	700.68 (Ref. 23)
C^{2+}	$1s2p^3$	$^5S^o$	688.83	688.08 (Ref. 23)
C^{2+}	$1s2s2p3s$	$^5P^o$	671.6	
C^{2+}	$1s2s2p3s$	^5S	668.97	
		^5P	668.62	
		^5D	669.54	
C^{2+}	$1s2s2p3d$	$^5P^o$	661.1	
C^{3+}	$1s2s3s$	^4S	612.79	612.73 (Ref. 21)
				612.79 (Ref. 22)
C^{3+}	$1s2s3p$	$^4P^o$	610.1	
C^{3+}	$1s2s3d$	^4D	608.4	
C^{3+}	$1s2p3p$	^4S	603.7	603.77 (Ref. 22)
		^4P	604.6	
		^4D	604.9	
C^{3+}	$1s2p3d$	$^4D^o$	602.3	

[a]Energies are given above for the corresponding ground state.

multiconfiguration expansion, whereas external correlation was added as an empirical correction due to Sinanoğlu.[20]

The calculated energies are given in Table I. Their accuracy is slightly smaller or larger than 0.1 eV, as indicated in the table. We note that the agreement with the CI energies of Holøien and Geltman[21] and Larsson *et al.*[22] is good. Safronova's and Kharitonova's values[23] based on the first three terms of the Z^{-1} expansion are 0.5 to 1 eV too low indicating that more expansion terms are necessary for $Z=6$.

IV. SPECTROSCOPIC ASSIGNMENTS

In Fig. 2 a prompt 400-keV C^+ on CH_4 spectrum is shown at a larger scale. Since the target region is viewed directly by the electron spectrometer, prompt Auger transitions (lifetime $\tau \lesssim 10^{-10}$ sec) are measured. However, due to the finite time resolution of the analyzer a small fraction of metastable autoionizing carbon states ($\tau \gtrsim 10^{-10}$ s) is observed as well.

From the spectroscopic assignment given in Refs. 7 and 9 the prompt Auger structures labeled 1 to 11 are mainly attributed to singly core-excited Li-, Be-, and B-like initial electron configurations. Owing to a large number of possible state combinations in three-to-five electron systems the prompt carbon spectrum is a compo-

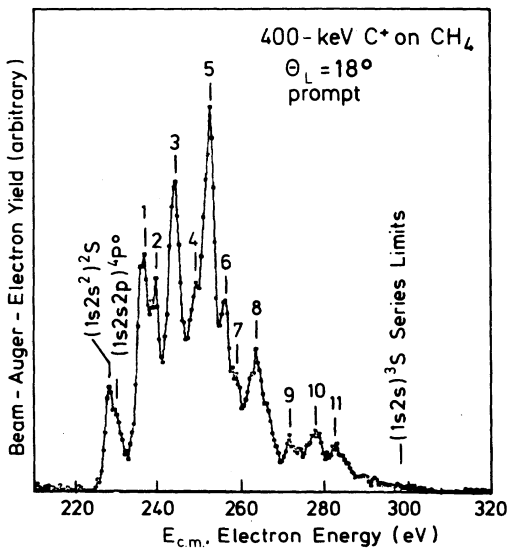

FIG. 2. Prompt carbon projectile Auger spectrum excited in 400-keV C^+ on CH_4 collisions.

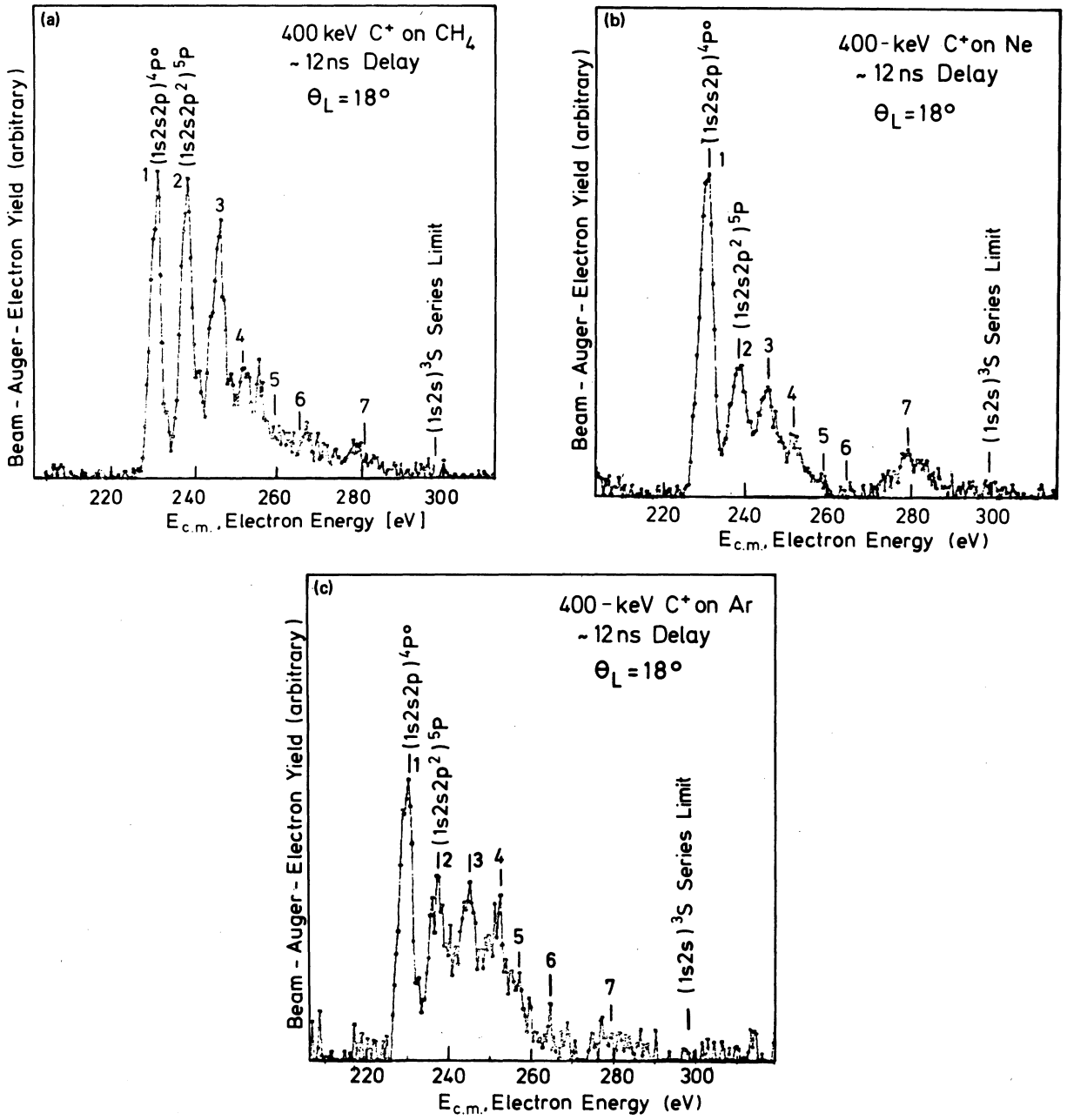

FIG. 3. Delayed carbon Auger spectra excited in 400-keV C^+ on Ne, Ar, and CH_4 collisions. (a) C^+ on CH_4, (b) C^+ on Ne, and (c) C^+ on Ar. Calibration of ionic rest frame energies ($E_{c.m.}$) was achieved by using a transition energy of 229.7 eV for the C IV $1s2s2p\,^4P^o$ state (see Fig. 4).

sition of many lines. The complexity of the observed prompt spectrum is further increased due to Auger cascades subsequent to beam-gas excitation. Thus in many cases Auger cascades lead to core-excited states of the next higher ionization stage which in turn decay to lower-lying states by Auger processes or via radiative transitions. Such cascade mechanisms possible cause a drastic repopulation of initial projectile states within some hundred Angströms of flight path.

The first peak in Fig. 2 at about 228 eV is attributed to the formation of core-excited $1s2s^2\,^2S$ and $1s2s2p\,^4P^o$ states in C IV. Recently, it has been demonstrated that gaseous targets such as CH_4 give high-excitation probabilities for metastable autoionizing states.[8-10] It is further sug-

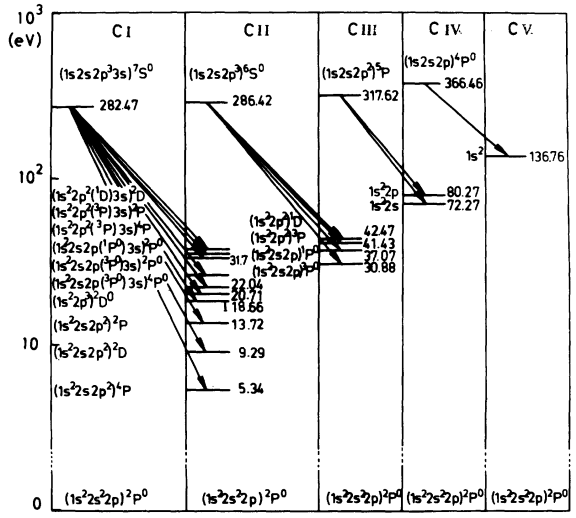

FIG. 4. Partial energy-level diagram representing autoionizing decays of the $^4P^o(1)$, $^5P(1)$, $^6S^o(1)$, and $^7S^o(1)$ terms in carbon. Autoionization transitions are indicated by arrows. The excitation energies (this work) are given above the $1s^22s^22p\ ^2P^o$ ground state in C II. The $1s^22p^23s\ ^4P$ energy level is calculated.

gested that the main spectral features in Fig. 2 (peak 1 to 8) originate from the decay of singly core-excited three-to-five electron carbon ions. The highest-energy group of lines in the prompt carbon spectrum (peak 9 to 11) is supposed to arise from Li-like $1s2lnl'$ configurations with one outer nl' electron being excited into the $n=3$ shell or higher. It is expected that initial C III $1snln'l'n''l''$ ($n,n',n'' \geq 3$) states cascade through Li-like states by Auger-electron emission. Thus, four-electron systems such as $1s3s^2nl$, $1s3s3pnl$, and $1s3p^2nl$ in C III can make significant contributions to core-excited states in C IV. The reorganization of C III $1snln'l'n''l''$ states may occur in two stages as follows:

(a) Auger transitions populating an intermediate state, for example, C III $(1s3s^2nl) \rightarrow$ C IV $1s2snl + \epsilon s$.

(b) The intermediate "cascade-fed" excited state subsequently decays again by an Auger transition, e.g., C IV $1s2snl \rightarrow$ C V $1s^2 + \epsilon l$.

Some of the intensity in the area above 270 eV (see Fig. 2) could also be attributed to doubly core-excited states in C V, C IV, C III, and C II. The probability for a double K-shell ionization is, however, considered to be small at the impact energy of 400 keV.[9] At $E_{c.m.} = 298.96$ eV (corresponding to the C IV $1s2s\ ^3S \infty l - 1s^2\epsilon l$ series limit) the drop in intensity indicates that many of the Li-like states observed converge to this limit. Above this limit no pronounced structures exist.

At 400-keV beam-energy core-excited levels belonging to the charge states 1 and 2 should dominate. However, inspection of Figs. 1 and 2 clearly demonstrates also that Li-like states corresponding to the charge state 3 are created with considerable yield. From the prompt spectra ratios of intensities for three- to four-, and five-electron configurations were estimated. It is found that they are largest for the collision systems C^+ on Ne and smallest for C^+ on CH_4, i.e., multiple ionization increases as targets are used in the order of CH_4, Ar, and Ne. This striking effect is consistent with the delayed spectra which are discussed in the following.

Owing to specific selection rules[6,11,24,25] the time-delayed Auger-spectra displayed in Fig. 3 are less complicated than the prompt spectra (Figs. 1 and 2) with the target in view of the electron spectrometer. Our experimental results exhibit four pronounced peaks, which can be attributed mainly to autoionization of the $1s2s2p\ ^4P^o = {}^4P^o(1)$, $1s2s2p^2\ ^5P = {}^5P(1)$, $1s2s2p^3\ ^6S^o = {}^6S^o(1)$, and $1s2s2p^3 3s\ ^7S^o = {}^7S^o(1)$ states. The decay modes of these lowest-lying levels are shown in Fig. 4. For the most prominent lines peak energies are determined by fitting Gaussian line profiles using a least-square procedure. These energy values are listed in Table II together with previous experimental and theoretical data.[26-29]

In the delayed spectra the energetically lowest-lying line is identified as resulting from the metastable autoionizing state $1s2s2p\ ^4P^o$ in C IV. The energy scale in the center-of-mass (c.m.) frame was established by assigning a value of 229.7 eV to the $1s2s2p\ ^4P^o$ peak.[9] We further note that the peak at 237.4 eV is associated with the Auger decay of the $1s2s2p^2\ ^5P$ term in C III. The third strong peak at about 244.4 eV is due to autoionization of the $1s2s2p^2\ ^5P$ state in C III and the $1s2s2p^3\ ^6S^o$ state in C II. Peak 4 is attributed mainly to Auger decays originating from the $^6S^o(1)$ levels in C II. The remaining less intense features (labeled 5 to 6) towards higher energy are assigned as transitions arising predominantly from $^6S^o(1)$ and $^7S^o(1)$ carbon states. The feature labeled 6 is most pronounced for the collision system C^+ on CH_4 [see Fig. 3(a)]. We further note that a broad structure (labeled 7) coincides with transition energies for C IV $1s2l3l'$ and C IV $1s2l4l'$ Rydberg states (see Table II). As can be seen from Fig. 3(b) this structure is enhanced for the C^+ on Ne collision system.

The intensity ratio of the $1s2s2p\ ^4P^o$ line to the total intensity reveals an enhancement for C^+ on Ne compared to the other delayed spectra. This effect may possibly be explained by feeding mechanisms through cascading decay of highly excited three- and four-electron configurations via optical and autoionization transitions into the meta-

TABLE II. List of predicted Auger-transition energies of several high-spin states in C I, C II, C III, and C IV. Comparison is made with experimental peak energies of the most prominent lines in Fig. 3. Earlier experimental and theoretical values are also listed.

Initial charge state	Initial state	Final ionic state	Transition energy (eV) Theory	Transition energy (eV) Other Experiments	Peak number (Fig. 3)	Peak energy (eV) This work	Assignment	Comment
C^{3+}	$1s2s2p\ ^4P^o$	$1s^2\ ^1S$	229.72[a] 229.82[b]	229.7 ± 0.5[c] 229.9 ± 1[d]	1	229.7[j]	C IV $1s2s2p\ ^4P^o$	Population of the C IV $1s2s2p\ ^4P^o$ states due to cascade-feeding processes
C^{2+}	$1s2s2p^2\ ^5P$	$1s^22p\ ^2P^o$	237.35[e] 237.45[d]	238 ± 1[d]				Population of the C III $1s2s2p^2\ ^5P$ states due to cascade-feeding processes
C^{3+}	$1s2p^2\ ^4P$	$1s^2\ ^1S$		238.9[f,j]	2	237.4 ± 0.5	C III $1s2s2p^2\ ^5P$	
C^+	$1s2s2p^3\ ^6S^o$	$1s^22p^2\ ^1D$	243.95[d]					
C^+	$1s2s2p^3\ ^6S^o$	$1s^22p^2\ ^3P$	245.00[d]		3	244.4	C II $1s2s2p^3\ ^6S^o$ C III $1s2s2p^2\ ^5P$	
C^{2+}	$1s2s2p^2\ ^5P$	$1s^22s\ ^2S$	245.35[e] 245.45[d]	245 ± 1[d]				
C^+	$1s2s2p^3\ ^6S^o$	$1s^22s2p\ ^1P^o$	249.35[e,d]		4	251.4	C II $1s2s2p^3\ ^6S^o$ C I $1s2s2p^3 3s\ ^7S^o$	
C^{2+}	$1s2p^3\ ^5S^o$	$1s^22p\ ^2P^o$	249.58[e]					
C^+	$1s2s2p^3\ ^6S^o$	$1s^22s2p\ ^3P^o$	255.54[e,d]					
C^{2+}	$1s2p^3\ ^5S^o$	$1s^22s\ ^2S$	257.58[e]		5	258.1	C II $1s2s2p^3\ ^6S^o$ C I $1s2s2p^3 3s\ ^7S^o$	
C	$1s2s2p^3 3s\ ^7S^o$	$1s^22s2p\ ^3P^o\ 3s\ ^2P^o$	260.43[d]					
C	$1s2s2p^3 3s\ ^7S^o$	$1s^22s2p\ ^3P^o\ 3s\ ^4P^o$	261.77[d]					
C	$1s2s2p^3 3s\ ^7S^o$	$1s^22p^3\ ^2D$	263.82[d]		6	264.2	C I $1s2s2p^3 3s\ ^7S^o$	Pronounced for the collision system C → CH_4
C	$1s2s2p^3 3s\ ^7S^o$	$1s^22s2p^2\ ^2P$	268.75[d]					
C^{3+}	$1s2s3s\ ^4S$	$1s^2\ ^1S$	269.26[e] 269.26[b] 269.32[g]	269.1[f,j]				
C^{3+}	$1s2s3p\ ^4P^o$	$1s^2\ ^1S$	271.95[b] 272.06[h] 272.28[g]	272.1[f,j]				

TABLE II. (*Continued*).

Initial charge state	Initial state	Final ionic state	Transition energy (eV) Theory	Transition energy (eV) Other Experiments	Peak number (Fig. 3)	Peak energy (eV) This work	Assignment	Comment
C	$1s2s2p^3 3s\ ^7S^o$	$1s^2 2s2p^2\ ^2D$	273.18[d]					
C^{3+}	$1s2s3d\ ^4D$	$1s^2\ ^1S$		273.4[f,j]				
C^{3+}	$1s2p3s\ ^4P^o$	$1s^2\ ^1S$	275.85[b]	275.7[f,j]				
C	$1s2s2p^3 3s\ ^7S^o$	$1s^2 2s2p^2\ ^4P$	277.14[d]					
C^{3+}	$1s2p3p\ ^4S$	$1s^2\ ^1S$	278.28[b]				Mainly Li-like quartet states of the type C IV $1s2l3l'$ and C IV $1s2l'4l'$	Broad structure most pronounced for the collision system $C^+ \rightarrow Ne$
C^{3+}	$1s2p3d\ ^4P^o$	$1s^2\ ^1S$	281.92[b]		7 ~ 280			
C^{3+}	$1s2s4s\ ^4S$	$1s^2\ ^1S$	283.49[b]	283.3[f,j]				Population of the $1s2131'$ and $1s2141'$ quartet states due to cascade-feeding processes
C^{3+}	$1s2s4p\ ^4P^o$	$1s^2\ ^1S$	284.46[b]					
	$1s2s2p^2\ ^5P \infty l$ Series limit	$1s^2 2p^2\ ^1D$	275.2[e]					
	$1s2s2p^2\ ^5P \infty l$ Series limit	$1s^2 2p^2\ ^3P$	276.2[e]					
	$1s2s2p^2\ ^5P \infty l$ Series limit	$1s^2 2s2p\ ^1P^o$	280.6[e]					
	$1s2s2p\ ^4P^o \infty l$ Series limit	$1s^2 2p\ ^2P^o$	286.2[e]					
	$1s2s2p^2\ ^5P \infty l$ Series limit	$1s^2 2s2p\ ^3P^o$	286.7[e]					
	$1s2s2p\ ^4P^o \infty l$ Series limit	$1s^2 2s\ ^2S$	294.2[e]					No structure observed above the $1s2s\ ^3S \infty l$ series limit
	$1s2s\ ^3S \infty l$ Series limit	$1s^2\ ^1S$	298.86[i]					
	$1s2p\ ^3P \infty l$ Series limit	$1s^2\ ^1S$	304.42					

[a] Vainshtein *et al.* (Ref. 26).
[b] Larsson *et al.* (Ref. 22).
[c] Rødbro *et al.* (Ref. 9).
[d] Schneider *et al.* (Ref. 7).
[e] This work.
[f] To *et al.* (Ref. 27).
[g] Holøien and Geltman (Ref. 21).
[h] Samanta and Ali (Ref. 28).
[i] Bashkin and Stoner (Ref. 29).
[j] The absolute energy scale is calibrated using the C IV $1s2s2p\ ^4P^o$ term energy of Rødbro *et al.* (Ref. 9).

stable $1s2s2p\,^4P^o$ state. A typical cascade process is illustrated in Fig. 5. It is seen from Fig. 5 that the C III $1s3s^24p\,^3P^o$ terms can decay via Auger effect to the $1s2s4p\epsilon s\,^3P^o$ continuum, while the residual $1s2s4p\,^4P^o$ state in C IV is depleted mainly via $E1$ transitions, thus populating in the next step the $1s2s3s\,^4S$ state, which in turn feeds the $1s2s2p\,^4P^o$ state. Such cascade processes appear to be strong candidates for the population of the $1s2s2p\,^4P^o$ states in C IV.

Another interesting situation may occur if core-excited states of the type $1s2snl\,^4L$ with high orbital and angular-momentum quantum number nl are created during the excitation process. For example, the so-called Yrast levels[30,31] of smallest $n=l+1$ decay through a succession of optical $\Delta n=\Delta l=1$ transitions during their time of flight. A characteristic multistage cascade process is illustrated in Fig. 6. This also can be an explanation for the population of the lowest-quartet states in C IV. If, however, two electrons in the initial core-excited state have antiparallel spin, autoionization will dominate; for instance,

$$1s2snl\ ^2L \rightarrow 1s^2+\epsilon l\,.$$

V. TOTAL CROSS SECTIONS AND RELATIVE INTENSITIES

An electron observation angle of 18° relative to the beam axis was used, so that in all cases the kinematically (Doppler-) shifted Auger peaks were well separated from the target peaks. The Auger lines of the prompt spectra are superimposed on a continuous background of electrons. The shape of the background was determined from measurements of electrons at energies well above and below the Auger structure and by fitting the logarithm of the continuum cross section with a second-order polynomial. The background could then be subtracted from the spectra. The remaining Auger-electron intensity (Figs. 1 and 2) was integrated and the total cross section for Auger-electron production via K-shell ionization in the different collision systems was obtained.[15] From previous measurements it can be assumed here that the Auger electrons are emitted nearly isotropically.[32] Thus, in general, it was sufficient to detect the secondary electrons at one angle and to multiply by 4π to perform the angular integration. The spectra were corrected for anisotropy caused by the collision kinematics. The relationship[15,17] $I/I'=E/E'$ between Auger intensities I and I' per solid angle and the corresponding centroid energies E and E' in the laboratory frame and the rest frame of the emitter, respectively, was used. Contributions from competing x-ray transition were neglected. Thus the integrated intensities in the different prompt Auger spectra are set equal to the corresponding cross sections for K-shell ionization in carbon projectile atoms. Also, Auger electrons produced via higher-order effects were neglected in the analysis.[33]

Absolute K-vacancy production cross sections are listed in Table III. In Fig. 7 they are plotted

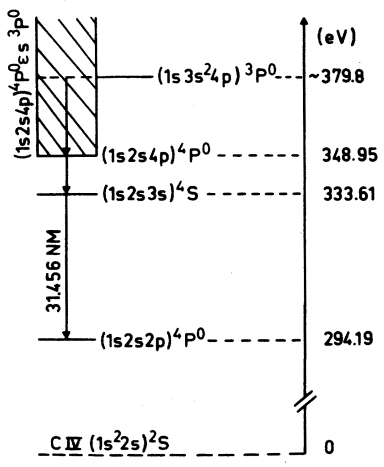

FIG. 5. Example for a cascade process of $1s3s^24p\,^3P^o$ terms in C III leading possibly to an overpopulation of the $1s2s2p\,^4P^o$ state.

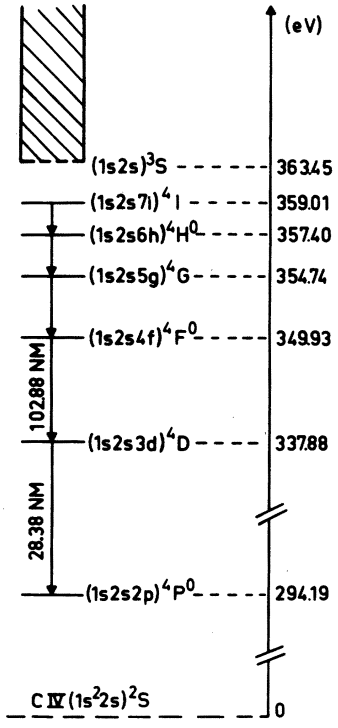

FIG. 6. Population of the $1s2s2p\,^4P^o$ state in C IV through a sequence of optical cascades. Transitions of the type $\Delta n=1$ and $l=n-1$ are indicated.

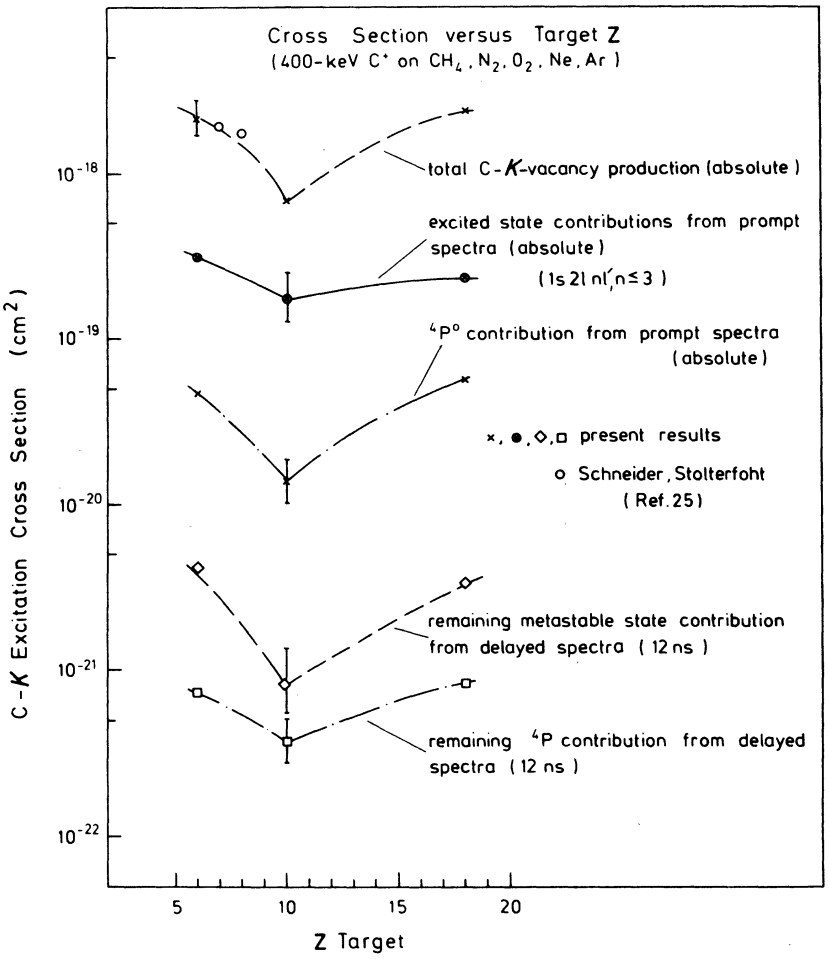

FIG. 7. Absolute K-vacancy-production cross sections in carbon versus Z from collisions of 400-keV C^+ on CH_4, N_2, O_2, Ne, and Ar deduced from prompt Auger spectra. The total K-vacancy-production cross section are compared to cross sections for production of initial configurations with highly excited states ($1s2lnl'$, $n \geq 3$) with intensities between 270 and 300 eV. In addition, relative cross sections for metastable states after a time delay of 12 ns are plotted for comparison.

versus target Z. We note that K-shell excitation cross sections for carbon at higher and lower impact energies have been published recently.[34,35] The upper curve (Fig. 7) gives the total absolute cross sections for K-vacancy production in carbon as a function of different exciter gases for carbon projectile ions at an impact energy of 400 keV.

In addition to total cross sections we studied cross sections of individual Auger lines. Thus, from the prompt high-resolution spectra (Figs. 1 and 2) the contribution of the $^4P^o$ state was deduced after a line fit and peak integration (Table III). The relative numbers for the contribution of the metastable states after a time delay of 12 ns were obtained after integration of the corresponding line in the delayed spectra [Figs. 3(a), 3(b), and 3(c)].

Owing to the differential metastability,[21,36,37] the $^4P^o(1)$ fine-structure components $J=\frac{1}{2}$, $\frac{3}{2}$, and $\frac{5}{2}$ decay at different rates, where the $J=\frac{5}{2}$ state has a larger lifetime than the corresponding $J=\frac{1}{2}$ and $\frac{3}{2}$ ones. In principle, the mean lifetime of the $1s2s2p\,^4P^o$ state can be obtained by measuring its intensity as a function of delay time.[38,39] In this work lifetime measurements were limited for the following reasons: Owing to strong cascades significant departure from exponential decays was observed. In such cases the intensity of observed decay profiles varies in quite a complicated way. On the other hand, lifetime measurements of the long-lived $^4P^o_{5/2}$ level were hampered by the finite length of the gas-jet-translation mechanism.

In order to deduce cross sections for the $^4P^o(1)$ state in CIV an estimated mean decay constant of about 20 ns (this value is an average value with

TABLE III. Absolute K-vacancy-production cross sections and relative cross sections for remaining metastables as deduced from prompt and time-delayed (12 ns) electron emission spectra from 400-keV C^+ on CH_4, Ne, and Ar collisions.

Exciter gas	Cross sections deduced from prompt spectra: Total K-shell vacancy-production cross sections in carbon (10^{-20} cm^2)	Cross sections deduced from prompt spectra: Partial production cross section for $1s2s2p\ ^4P^o$ in carbon (10^{-20}cm^2)	Relative cross sections deduced from time-delayed spectra 12 ns: Relative cross sections for remaining metastable components in carbon beam (10^{-22} cm^2)	Relative cross section for $1s2s2p\ ^4P^o$ in carbon beam (10^{-22} cm^2)
CH_4	214	4.9[a]	42.6	7.4
Ne	69	1.36[a]	8.6	3.8
Ar	240	5.81[a]	34.2	8.1
	(error ± 15%)	(error ± 40%)	(error ± 40%)	(error ± 40%)

[a] Corrected for finite viewing region of spectrometer (Ref. 44) using a mean lifetime for $^4P^o$ of 20 ns.

respect to the different J components) was introduced. We note that Chang *et al.*[40] calculated a lifetime of 88.3 ns for the $^4P^o_{5/2}$ state, whereas Balashov *et al.*[41,42] obtained 111 ns. Finally, Dmitriev[43] deduced a value of 11.3 ns using foil excitation. We further note that our deduced line intensities for the $^4P^o(1)$ peak are corrected for the decay within the finite observation length of the spectrometer.[44] However, the uncertainty in the used average lifetime (20 ns) causes a large uncertainty in these numbers. These numbers should be understood as a sum of cross-section component $\sigma_T(^4P^o)$ resulting from the "natural" decay of the $^4P^o$ state and a cross-section component $\sigma_C(^4P^o)$ due to cascade feeding; possible cascades are indicated in Figs. 5 and 6. The relative cross section $\sigma_D(^4P^o)$ at a certain delay time is therefore given as $\sigma_D = \sigma_T + \sigma_C$. σ_T is related to the production cross section for the $^4P^o$ state by its mean lifetime. Uncertainties for σ_C cross sections are mainly due to the unknown initial population of the high-lying Rydberg states.

The error for the absolute total cross sections given in Fig. 7 and Table III is about (±15%). This error is primarily caused by uncertainties in the determination of the target-gas pressure and the detector efficiency calibration. The relative uncertainties in the cross sections with respect to the variation of the projectile energy are typically 10% due to counting statistics, beam integration, and background subtraction. The values for the metastable contributions are given within a large error of about (± 40%). This error is also due to an unknown contamination from prompt autoionizing transitions in the viewing region of the spectrometer and due to uncertainties in the lifetime determination.

Comparison of the total K-shell vacancy-production cross sections with the contributions for the $^4P^o$ state in carbon show nearly the same trend for the different exciter gases. However, specific spectral features are quite different in the case C^+ on Ne compared to the other two cases. For the investigated collision systems the K-shell vacancy production in carbon is mainly due to certain couplings between molecular orbitals (MO) which are formed in the quasimolecule during the collision.[32,33] Hence, vacancy production and electron excitation in the collision systems C^+ on CH_4 and C^+ on Ne may be explained as follows[32]: Vacancies which are produced in the $2p\pi$ MO at large internuclear distances are transferred from the $2p\pi$ to the $2p\sigma$ MO at smaller internuclear distances via rotational coupling. Especially in the case of carbon, a significant portion of the $2p\pi$ vacancies is thus transferred to the K shell of the carbon ion as it has been discussed in more

TABLE IV. Internuclear distances (R_K) for K-vacancy production in carbon ions incident on CH_4, Ne, and Ar (Refs. 32 and 33). R_K denotes the distances where vacancy transfer is due to rotational or radial coupling, respectively.

Exciter gas	R_K (a.u.)
CH_4	0.1 (rot. coupling)
Ne	0.03 (rot. coupling)
Ar	0.8 (rad. coupling)

detail, e.g., in Ref. 32, previously. In the collision system C^+ on Ar vacancies are produced in the Ar-L shell in the incoming part of the collision via electron promotion along the $3d\sigma$ MO (see Ref. 33). Then in the outgoing part of the collision at larger internuclear distances, vacancies can be transferred from the $3d\sigma$ MO into the $1s\sigma$ MO.[33] In Fig. 7, vacancy-production cross sections are plotted versus the atomic numbers Z of the corresponding collision partners. The dip in the cross-section curve of about $Z=10$ and the increase towards higher Z's can be understood from "level-matching" arguments.[33]

As indicated above, the K-vacancy production in carbon via the different couplings between different MO's due to the different targets occurs at different internuclear distances R_K. Those can be estimated from calculated MO diagrams or from cross sections as shown, e.g., in Refs. 32 and 33. The relevant distances for the K-shell ionization in carbon are given for comparison in Table IV.

It can be seen that the K-vacancy production in carbon takes place at a closer internuclear distance in the case where Ne is used as a target gas. This comparatively deeper interpenetration is not sufficient alone to explain the observed results. It is clear that additional processes, such as rearrangements and/or promotion of the outer electrons, should play an important role.

It can be noted from a comparison of the prompt spectra in Fig. 1 that the structure between 270 and 300 eV, which can be attributed to Li-like initial three-electron configurations of the type $1s2lnl'$ with $n \geq 3$, is very much favored in the case where Ne is used as an exciter gas. This is shown by the Z dependence of the cross sections for the production of these highly excited states as plotted in Fig. 7. These states are produced more frequently in C^+ on Ne collisions than in the other collision systems.

A comparison with the cross sections for the metastable contributions obtained from the delayed spectra, shows a similar target-Z dependence (see Table V). In fact the $^4P^o(1)$ line and the $1s2lnl'$ quartet states with $n \geq 3$ [see also Figs. 3(a), 3(b), and 3(c)] are most pronounced for C^+ on Ne impact. That should cause a strong "repopulation" of the $^4P^o$ state via cascade feeding. This is also seen but less strongly in the case where CH_4 or Ar are used as exciter gases. Thus the comparison of the measured spectra (Figs. 1, 2, and 3) and the cross sections suggests that the enhanced population of highly excited states in Ne is responsible for the strong population of the $^4P^o$ state. Another striking feature is the increased population of quintet and sextet states (see Figs. 1 and 3 and Table V), especially for C^+ on CH_4 collisions. Possible cascade-feeding mechanisms of ^5L terms in C III and ^6L terms in C II are discussed in Sec. VI.

VI. GROTRIAN DIAGRAMS FOR C III QUINTET AND C II SEXTET TERMS

Metastable autoionizing ^4L, ^5L, ^6L, and ^7L states other than the lowest-lying one of a given term system can cascade into the lowest-quartet, -quintet, -sextet, or -septet state by electric-dipole radiation. The lifetimes of such states will then be determined by the decay rates for both $E1$ transitions and autoionization. Let us consider

TABLE V. Relative intensities for the most prominent metastable autoionizing states after a time delay of 12 ns [see Figs. 3(a), 3(b), and 3(c)]. The relative intensities are deduced after performing a Gaussian line fit and are normalized to peak 1 in Fig. 3. The error for the relative intensities is (±40%).

	Relative peak intensities (Figs. 3) (normalized to $1s2s2p\,^4P^o$)					
System (400 keV)	$1s2s2p\,^4P^o$ (229.7 eV) Peak 1	$1s2s2p^2\,^5P$ (237.4 eV) Peak 2	(244.4 eV) Peak 3	(251.4 eV) Peaks 4 and 5	(264.2 eV) Peak 6	(281 eV) Peak 7
C^+ on CH_4	1	0.72	0.78	0.57	0.21	0.2
C^+ on Ne	1	0.45	0.36	0.22	0.01	0.26
C^+ on Ar	1	0.56	0.56	0.44	0.2	0.16

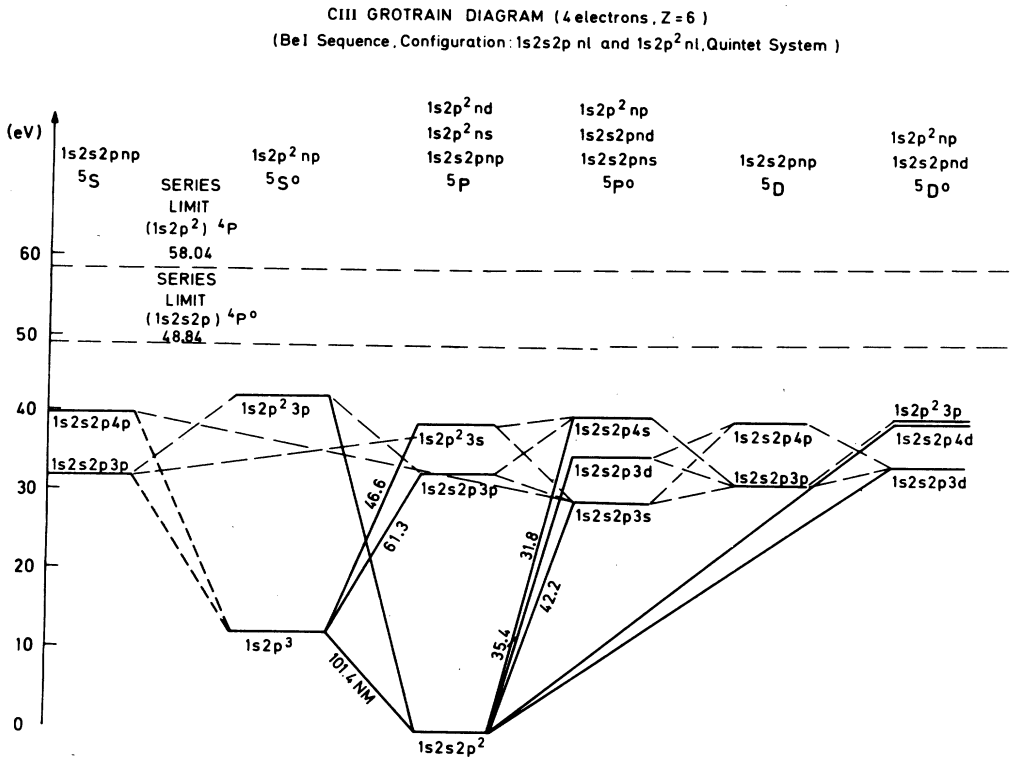

FIG. 8. The C III quintet system. The wavelengths of transitions are given in nanometers. Estimated accuracy 0.2 to 0.5%.

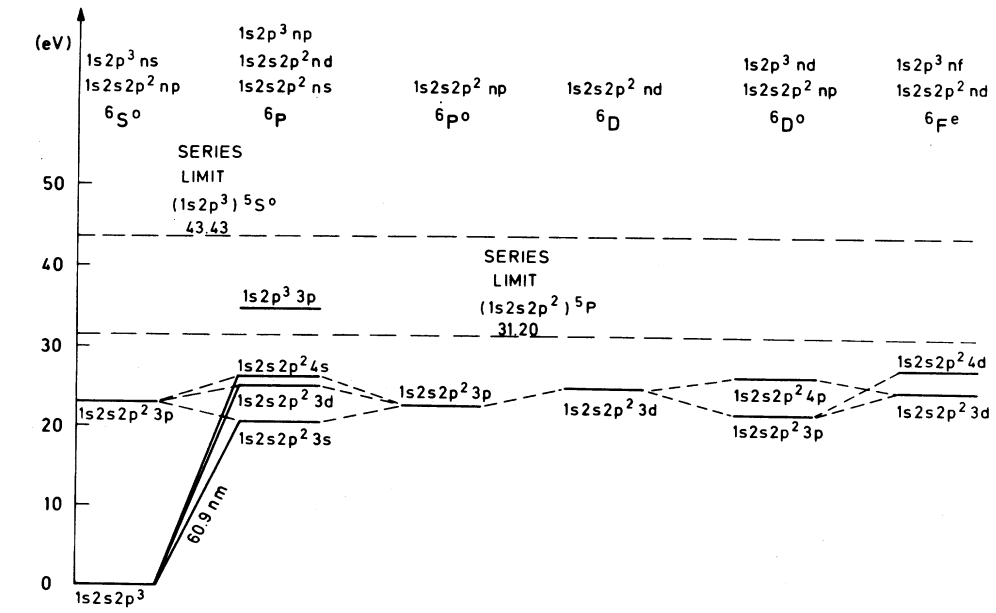

FIG. 9. The C II sextet system. Accuracy of the wavelength is ~0.1 nm.

first the decay of Be-like quintet states in C III. In Fig. 8 we suggest the corresponding Grotrian diagram. The deduced wavelengths as indicated in Fig. 8 were based on the theoretical data given in Table I. Quintet terms below the $1s2s2p\,^4P^o$-series limit at about 48.84 eV should dominantly decay via $E1$ transitions. For the decay of the transition $1s2s2p^2\,^5P$-$1s2p^3\,^5S^o$ we predict a wavelength of about 101.4 ± 0.5 nm. Possible quintet autoionizing states with energies lying above the $1s2s2p\,^4P^o$-series limit will generally have shorter lifetimes, since Coulomb autoionization is allowed for them. Consequently these states do not make appreciable contributions to the time-delayed Auger spectra.

In Fig. 9 we show a sextet-term scheme of boronlike C II states. For the $1s2s2p^3\,^6S^o$-$1s2s2p^2 3s\,^6P$ transition we calculated a wavelength of about 60.9 ± 1 nm. It should be noted that sextet states above the $1s2s2p^2\,^5P$-series limit (see Fig. 9), such as $1s2p^3 3p\,^6P$, can Coulomb autoionize.

VII. CONCLUSION

In summary, it has been shown that "exotic" autoionizing and metastable states with several open shells and high multiplicity are created in single gas collisions. These core-excited states then may decay via a sequence of Auger decays and optical transitions. The final state of this cascade process is not necessarily the ground state of the resultant ion. It is therefore expected that many beam-gas created states are initially multiply excited. Furthermore, it is demonstrated that depending on the collision system, it is possible to influence the population or repopulation of certain metastable states via cascade feeding. Such cascade-feeding processes are, e.g., important when studying alignment.[45] Much of the initial anisotropy may be carried away by Auger-electron emission or optical cascades, thus reducing the anisotropy of the cascade-fed highly excited states. Furthermore, we have found evidence of strong population of quintet and sextet terms. Radiative transitions among such states are expected to occur, but have not been reported yet in the literature.

Finally, we emphasize that so far no calculation of cross sections of such high-spin states exist. In order to study the mechanisms by which these high-spin states are formed in more detail, the Auger and photon deexcitation of the carbon projectiles as well as the target atoms should be measured simultaneously.

ACKNOWLEDGMENTS

The authors wish to thank Professor J. H. Briggs, Dr. L. J. Dubé, and Dr. L. Kocbach for helpful comments.

*Present address: Fakultät für Physik, Universität Freiburg, D-7800 Freiburg, West Germany.

[1] H. G. Berry, J. Desesquelles, and M. Dufay, Nucl. Instrum. Methods 110, 43 (1973).
[2] H. G. Berry, Phys. Scr. 12, 5 (1975) and references quoted therein.
[3] H. G. Berry, Rep. Prog. Phys. 40, 155 (1977).
[4] R. Bruch, G. Paul, and J. Andrä, Phys. Rev. A 12, 1808 (1975).
[5] R. Bruch, G. Paul, and J. Andrä, J. Phys. B 8, L253 (1975).
[6] R. Bruch, thesis, Freie Universität Berlin, 1976 (unpublished).
[7] D. Schneider, R. Bruch, W. H. E. Schwarz, T. C. Chang, and C. F. Moore, Phys. Rev. A 15, 926 (1977) and references quoted therein.
[8] R. Bruch, M. Rødbro, P. Bisgaard, and P. Dahl, Phys. Rev. Lett. 39, 801 (1977).
[9] M. Rødbro, R. Bruch, and P. Bisgaard, J. Phys. B 12, 2413 (1979) and references quoted therein.
[10] R. Bruch, D. Schneider, W. H. E. Schwarz, M. Meinhart, B. M. Johnson, and K. Taulbjerg, Phys. Rev. A 19, 587 (1979).
[11] W. Mehlhorn (unpublished).
[12] D. Schneider and N. Stolterfoht, *Abstracts of the Tenth ICPEAC, Paris, 1977*, edited by M. Barat and J. Reinhardt (Commissariat à L'Energie Atomique, Paris, 1977), p. 1314.
[13] D. L. Matthews, R. Fortner, D. Schneider, and C. F. Moore, Phys. Rev. A 14, 1561 (1976).
[14] H. F. Beyer, R. Mann, F. Folkmann, K. H. Schartner, *Abstracts of the Eleventh ICPEAC, Kyoto, 1979*, edited by K. Takayanagi and N. Oda (The Society for Atomic Collision Research, Kyoto, 1979).
[15] N. Stolterfoht, D. Schneider, D. Burch, B. Aagaard, E. Bøving, and B. Fastrup, Phys. Rev. A 12, 1313 (1975); N. Stolterfoht, D. Schneider, K. G. Harrison, *ibid.* 8, 1363 (1973).
[16] N. Stolterfoht, H. J. Gabler, and U. Leithäuser, Phys. Lett. 45A, 5 (1973); 45A, 351 (1973).
[17] P. Dahl, M. Rødbro, B. Fastrup, and M. E. Rudd, J. Phys. B 9, 1567 (1976).
[18] W. H. E. Schwarz and T. C. Chang, Int. J. Quantum Chem. S 10, 91 (1976).
[19] T. C. Chang and W. H. E. Schwarz, Theor. Chim. Acta 44, 45 (1977).
[20] O. Sinanoğlu, At. Phys. 2, 131 (1969).
[21] E. Holøien and S. Geltman, Phys. Rev. 153, 81 (1967).
[22] S. Larsson, R. Crossly, and T. Ahlenius, J. Phys. (Paris) Colloq. C1, 40, 6 (1979).
[23] U. I. Safronova and V. N. Kharitonova, Opt. Spectrosc. (USSR) 27, 300 (1969).

[24]P. Feldman and R. Novick, Phys. Rev. 160, 143 (1967).
[25]H. J. Andrä, *Fast-Beam (Beam-Foil) Spectroscopy, Progress in Atomic Spectroscopy Part B*, edited by W. Hanle and H. Kleinpoppen (Plenum, New York, 1979), p. 829.
[26]L. A. Vainshtein and U. I. Safronova, At. Data Nucl. Data Tables 21, 49 (1978).
[27]K. X. To, E. Knystautas, R. Drouin, and H. G. Berry, J. Phys. (Paris) Colloq. C1, 40, 1 (1979).
[28]S. R. Samanta and M. A. Ali, J. Phys. B 11, 581 (1978).
[29]S. Bashkin and J. O. Stoner, Jr., *Atomic Energy Levels and Grotrian Diagrams* (North-Holland, Amsterdam, 1975).
[30]L. J. Curtis, J. Phys. 40, Colloq. C1, Suppl. No. 2, C1-139 (1979).
[31]S. Bashkin, *Beam-Foil Spectroscopy 1*, edited by I. A. Sellin and P. J. Pegg (Plenum, New York, 1976), p. 129.
[32]D. Schneider and N. Stolterfoht, Phys. Rev. A 19, 55 (1979); D. Schneider and N. Stolterfoht (unpublished).
[33]N. Stolterfoht (unpublished).
[34]M. Sakisaka, N. Maeda, H. Hori, and N. Kobayashi, J. Phys. B 12, 3569 (1979).
[35]N. Kobayashi, N. Maeda, H. Kojima, S. Yamada, and M. Sakisaka, J. Phys. B 12, 3579 (1979).
[36]M. Levitt, R. Novick, and P. D. Feldman, Phys. Rev. A 3, 130 (1971).
[37]A. E. Livingston and H. G. Berry, Phys. Rev. A 17, 1966 (1978).
[38]B. Donally, W. W. Smith, D. J. Pegg, M. Brown, and I. A. Sellin, Phys. Rev. A 4, 122 (1971).
[39]R. Bruch, G. Paul, and J. Andrä, J. Phys. B 8, L253 (1975).
[40]K. T. Cheng, C. P. Liu, and W. R. Johnson, Phys. Lett. 48A, 437 (1974).
[41]P. Feldman, M. Levitt, and R. Novick, Phys. Rev. Lett. 21, 331 (1968).
[42]V. V. Balashov, V. S. Senashenko, and B. Tekou, Phys. Lett. 25A, 487 (1967).
[43]I. S. Dmitriev, Ya. A. Teplova, and V. S. Nikolaev, Sov. Phys.—JETP 34, 723 (1972).
[44]W. W. Smith, B. Donnally, D. J. Pegg, M. Brown, and I. A. Sellin, Phys. Rev. A 7, 487 (1973).
[45]J. Macek, *Beam-Foil Spectroscopy, Vol. 2*, edited by I. A. Sellin and D. J. Pegg (Plenum, New York, 1975), p. 781.